

Article

Facile Synthesis of V₂O₅ Hollow Spheres as Advanced Cathodes for High-Performance Lithium-Ion Batteries

Xingyuan Zhang ¹, Jian-Gan Wang ^{1,*}, Huanyan Liu ¹, Hongzhen Liu ¹ and Bingqing Wei ^{1,2,*}

¹ State Key Laboratory of Solidification Processing, Center for Nano Energy Materials, School of Materials Science and Engineering, Northwestern Polytechnical University and Shaanxi Joint Lab of Graphene (NPU), Xi'an 710072, China; jackgs202@mail.nwpu.edu.cn (X.Z.); liuhuanyan@mail.nwpu.edu.cn (H.L.); liuhongzhennwpu@gmail.com (H.L.)

² Department of Mechanical Engineering, University of Delaware, Newark, DE 19716, USA

* Correspondence: wangjiangan@nwpu.edu.cn (J.-G.W.); weib@udel.edu (B.W.);
Tel.: +86-29-8846-0204 (J.-G.W.)

Academic Editor: Maryam Tabrizian

Received: 14 December 2016; Accepted: 16 January 2017; Published: 18 January 2017

Abstract: Three-dimensional V₂O₅ hollow structures have been prepared through a simple synthesis strategy combining solvothermal treatment and a subsequent thermal annealing. The V₂O₅ materials are composed of microspheres 2–3 μm in diameter and with a distinct hollow interior. The as-synthesized V₂O₅ hollow microspheres, when evaluated as a cathode material for lithium-ion batteries, can deliver a specific capacity as high as 273 mAh·g⁻¹ at 0.2 C. Benefiting from the hollow structures that afford fast electrolyte transport and volume accommodation, the V₂O₅ cathode also exhibits a superior rate capability and excellent cycling stability. The good Li-ion storage performance demonstrates the great potential of this unique V₂O₅ hollow material as a high-performance cathode for lithium-ion batteries.

Keywords: vanadium pentoxide; lithium-ion batteries; hollow spheres; cathode

1. Introduction

Rechargeable lithium-ion batteries (LIBs) are considered to be one of the most promising energy storage devices for portable devices and electric vehicles (EVs) owing to their high energy densities, environmental friendliness, and long cycle lifetime [1–4]. However, the challenges of high cost and the low capacity of the currently used cathode materials hinder their widespread applications [5,6]. In order to obtain high specific energy, considerable efforts have been devoted to developing materials with a higher specific capacity than the current commercial ones, such as LiCoO₂ (140 mAh·g⁻¹), LiMn₂O₄ (146 mAh·g⁻¹), and LiFePO₄ (176 mAh·g⁻¹) [7,8].

Among the alternative candidates, vanadium pentoxide (V₂O₅) has drawn considerable attention as a cathode material for lithium-ion batteries because of its advantages of layered structure, low cost, rich abundance in nature, and a high theoretical capacity of about 294 mAh·g⁻¹ (intercalation/deintercalation of two Li⁺ ions between 2.0 and 4.0 V) [9–11]. Nevertheless, the poor cycling stability, low electronic conductivity, and low lithium ion diffusion rate restrict its practical application [12–14]. Developing nanostructured materials has been demonstrated to be an effective method to address these critical issues because nanomaterials have a large surface area to provide more reaction sites and can effectively shorten the diffusion distance of lithium ions during the insertion/extraction, thereby resulting in an enhanced cycling performance and rate capability [15,16]. A variety of V₂O₅ nanostructures, such as nanourchins [17], nanotubes [18], nanospikes [10], nanorods [8], nanowires [19–21], and nanobelts [22–25], have been fabricated, and improved

electrochemical performance has been achieved with these materials when used as cathodes for LIBs. In particular, hollow structures are rather favorable because the unique hollow structure can effectively buffer the volume expansion of the V_2O_5 cathode to improve the cycling performance [9,26–28]. Lou et al. reported a carbon-templating method to synthesize V_2O_5 hollow spheres with an excellent electrochemical performance [9]. However, the complex synthesis procedures and the expensive reactant materials limit the scale-up production. Therefore, it remains a great challenge to controllably synthesize V_2O_5 hollow structures through a simple and low-cost method.

In this work, we report a facile one-step solvothermal method to controllably synthesize V_2O_5 hollow microspheres by employing a copolymer surfactant of poly(ethylene oxide)-block-poly(propylene oxide)-block-poly(ethylene oxide) (P123) as a soft template and low-cost NH_4VO_3 as the vanadium source. The effects of the annealing temperature on the crystallinity, morphology, and electrochemical properties of V_2O_5 have been studied. The optimized V_2O_5 hollow microspheres, when used as LIB cathodes, exhibit a satisfactory lithium-ion storage performance.

2. Discussion and Results

2.1. Structure and Morphology of the V_2O_5 Microspheres

Figure 1 shows the typical SEM images of the as-prepared samples. As shown in Figure 1a, the V_2O_5 precursor was composed of three-dimensional (3D) microspheres with diameters in the range of two to three microns. The magnified image in Figure 1a2 indicates that the microspheres were assembled with petal-like nanosheets. The hollow structure can be clearly observed in some broken microspheres (Figure 1a3). V_2O_5 was obtained by annealing the precursors, and the morphology evolution with the annealing temperature is exhibited in Figure 1b–d. The microsphere morphology was well maintained within the annealing temperature range of 300–500 °C. However, the building blocks changed with the temperature. At a low annealing temperature of 300 °C (V_2O_5 -300), as shown in Figure 1b2, the petal-like nanosheet structure was preserved on the V_2O_5 microsphere surface, which was almost identical to that of the precursors. As the temperature increased to 400 °C (V_2O_5 -400), the surface of the V_2O_5 hollow microspheres became constructed by interconnected nanoparticles (Figure 1c2). The nanoparticles became larger irregular structures at a higher temperature of 500 °C (V_2O_5 -500, Figure 1d2). The morphology evolution can be attributed to the different growth rate and crystallization degree of V_2O_5 at different annealing temperatures [27].

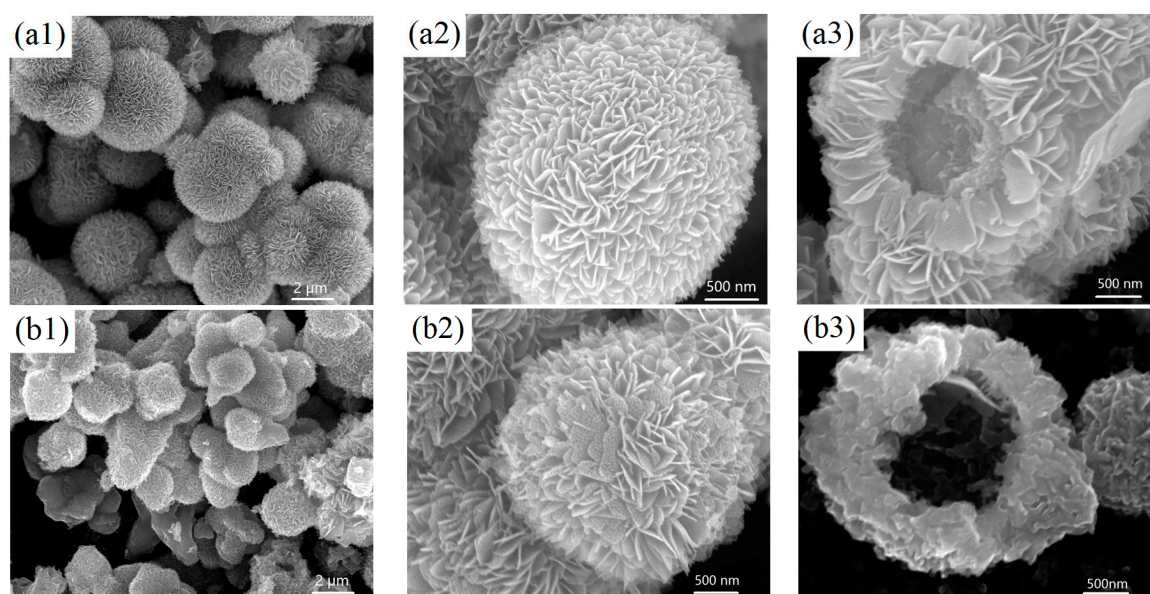


Figure 1. Cont.

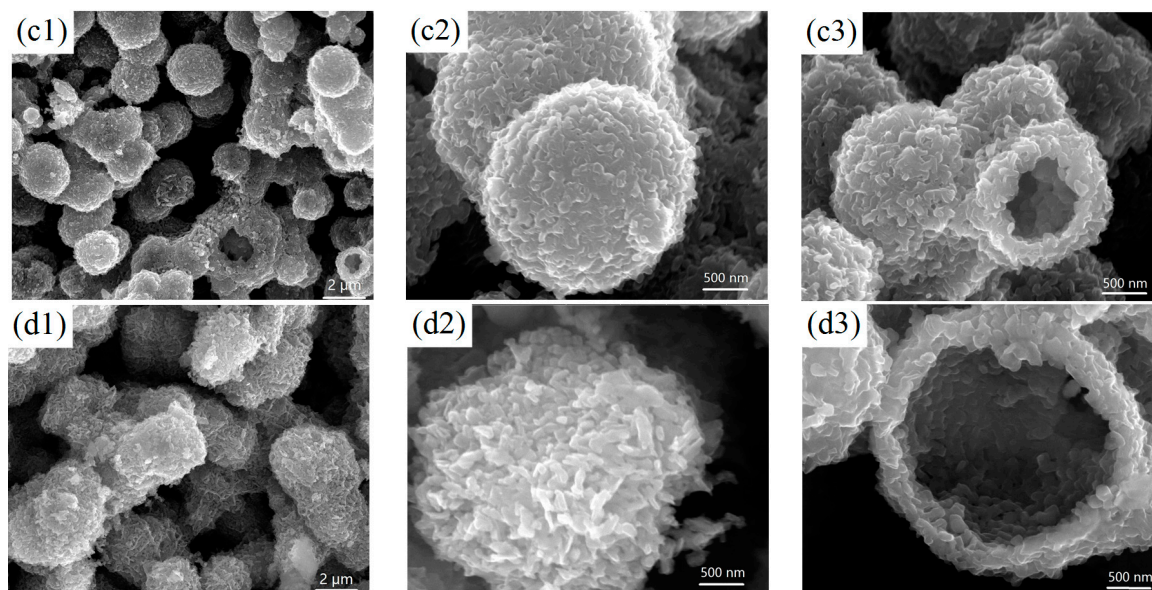


Figure 1. SEM images of the (a1–a3) V_2O_5 precursor and V_2O_5 microspheres annealed at 300 °C (b1–b3); 400 °C (c1–c3); and 500 °C (d1–d3).

The crystallographic structure of the samples was characterized by X-ray powder diffraction (XRD). Figure 2a shows the XRD patterns of V_2O_5 . Clearly, the main diffraction peaks can be well indexed to the orthorhombic phase of V_2O_5 (JCPDS Card No. 41-1426). In addition, the characteristic peaks showed a stronger diffraction intensity and narrower shape at an elevated annealing temperature, suggesting a higher crystallinity at a higher temperature [16,29]. Raman spectra were employed to further confirm the structure of the samples. As shown in Figure 2b, the samples shared identical Raman peaks, which are characteristic of orthorhombic V_2O_5 [29,30]. The typical Raman peaks V_2O_5 included the skeleton bent vibrations of the V–O–V bonds at 145 and 193 cm^{-1} , the bending vibration of the V=O bonds at 281 and 402 cm^{-1} , the bending vibrations of $V_3=O$ at 302 cm^{-1} and V–O–V bonds at 480 cm^{-1} , and the stretching vibrations of $V_3=O$ bonds at 527 cm^{-1} , $V_2=O$ bonds at 701 cm^{-1} , and V=O bonds at 995 cm^{-1} .

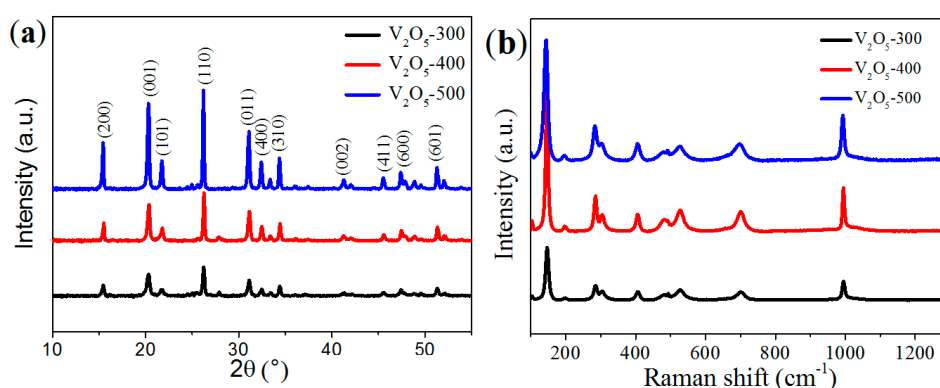


Figure 2. XRD patterns (a) and Raman spectra (b) of the V_2O_5 samples.

2.2. Electrochemical Performance

The electrochemical performance of the V_2O_5 samples was first evaluated using the cyclic voltammogram (CV). Figure 3 shows the first five CV curves of the V_2O_5 -400 cathode at a scan rate of 0.1 $mV \cdot s^{-1}$ in a potential range from 2.0 to 4.0 V. Four main pairs of redox peaks were observed at around 3.59/3.64, 3.36/3.45, 3.16/3.34, and 2.26/2.51 V, respectively, which are associated with

the reversible lithium intercalation/deintercalation into/from V_2O_5 to form $\alpha\text{-Li}_xV_2O_5$, $\varepsilon\text{-Li}_xV_2O_5$, $\delta\text{-Li}_xV_2O_5$, and $\gamma\text{-Li}_xV_2O_5$, as expressed in Equations (1)–(4) [25,26,31,32]. In addition, the CV curves were well overlapped, indicating the highly reversible reversibility and good cycling stability of the cathode.

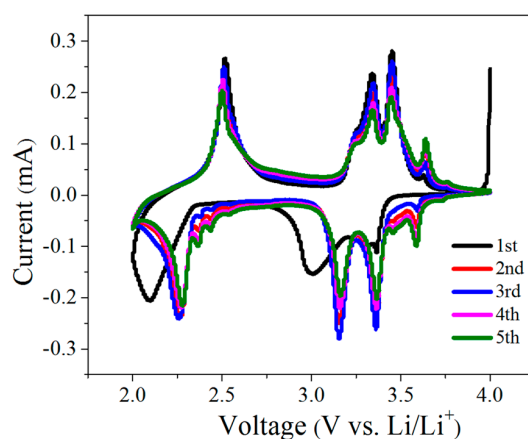
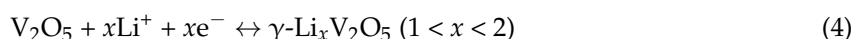
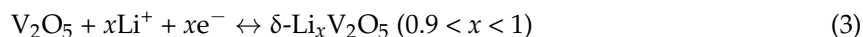
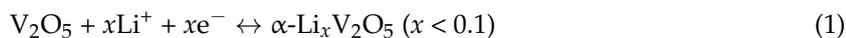


Figure 3. Cyclic voltammograms of V_2O_5 -400 cathode at a scan rate of $0.1 \text{ mV}\cdot\text{s}^{-1}$.

The electrochemical behavior of the V_2O_5 cathode was further investigated using the charge/discharge technique. Figure 4 exhibits the initial discharge/charge curves of V_2O_5 -300, V_2O_5 -400, and V_2O_5 -500 cathodes at a current density of 0.2 C ($1 \text{ C} = 300 \text{ mA}\cdot\text{g}^{-1}$). It is observed that the three cathodes share almost identical curve shapes, indicating a similar electrochemical behavior. More specifically, four voltage plateaus at around 3.58, 3.37, 3.18, and 2.26 V in the discharge curve correspond to the multi-step lithiation of V_2O_5 to form $\alpha\text{-Li}_xV_2O_5$, $\varepsilon\text{-Li}_xV_2O_5$, $\delta\text{-Li}_xV_2O_5$, and $\gamma\text{-Li}_xV_2O_5$, respectively, which is consistent with the CV analysis. The voltage plateaus clearly confirm the reverse-phase transformations in the discharge curve.

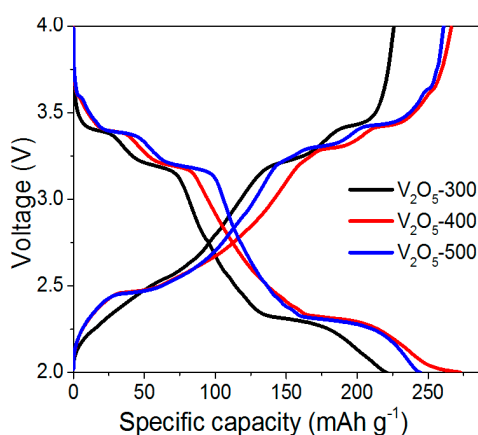


Figure 4. Charge-discharge curves of V_2O_5 -300, V_2O_5 -400, and V_2O_5 -500 cathodes.

The cycling performance of the hollow-structured V_2O_5 materials was examined using the galvanostatic charge/discharge test. As shown in Figure 5, all of the V_2O_5 cathodes exhibited

a reasonably good cycling performance over the 50 cycles at 0.2 C. It is important to note that the V_2O_5 -400 cathode delivers an initial discharge-specific capacity of $273 \text{ mAh}\cdot\text{g}^{-1}$, which is close to the theoretical value ($294 \text{ mAh}\cdot\text{g}^{-1}$). The specific capacity is also superior or comparable to most of the reported results based on differently structured V_2O_5 cathodes, such as the V_2O_5 nanorods ($272 \text{ mAh}\cdot\text{g}^{-1}$) [8], V_2O_5 hollow microspheres ($291 \text{ mAh}\cdot\text{g}^{-1}$) [9], V_2O_5 nanowires ($278 \text{ mAh}\cdot\text{g}^{-1}$) [16], V_2O_5 nanosheets ($272 \text{ mAh}\cdot\text{g}^{-1}$) [33] and $V_2O_5/\text{PEDOT}/\text{MnO}_2$ ($185 \text{ mAh}\cdot\text{g}^{-1}$) [21]. In addition, the initial specific capacity of the V_2O_5 -400 cathode was higher than that of V_2O_5 -300 ($221 \text{ mAh}\cdot\text{g}^{-1}$) and V_2O_5 -500 ($229 \text{ mAh}\cdot\text{g}^{-1}$), indicating that the annealing temperature exerts a considerable influence on the electrochemical performance. Moreover, the V_2O_5 -400 cathode retains a specific capacity of about $189 \text{ mAh}\cdot\text{g}^{-1}$ after 50 cycles.

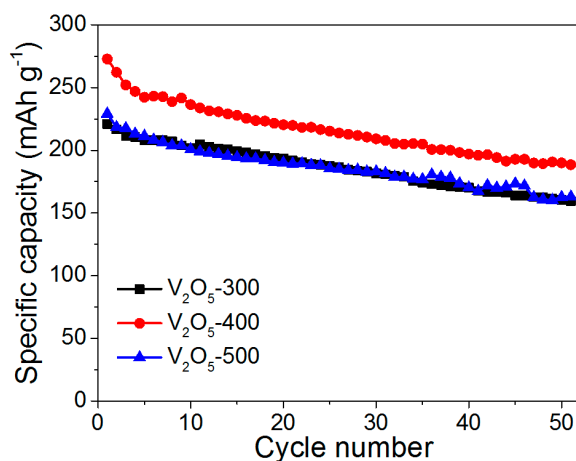


Figure 5. Cycling performance of V_2O_5 -300, V_2O_5 -400 and V_2O_5 -500 cathodes at 0.2 C.

In order to further demonstrate the performance of V_2O_5 hollow microspheres, the rate capability of the cathodes at different current rates was evaluated, as shown in Figure 6. As the current rate increased from 0.2 to 8 C, the V_2O_5 -400 cathode showed the smallest capacity decrease, indicating the best rate capability among the three cathodes. The discharge capacities of V_2O_5 -400 cathode at the current rates of 0.2, 0.5, 1, 2, 4, and 8 C were 256, 212, 198, 173, 144 and 114 $\text{mAh}\cdot\text{g}^{-1}$, respectively. Even after deep cycling at 8 C, the V_2O_5 -400 cathode could recover a specific capacity of about $210 \text{ mAh}\cdot\text{g}^{-1}$ when the current rate was returned to 0.2 C, further suggesting the good reactive reversibility of V_2O_5 -400.

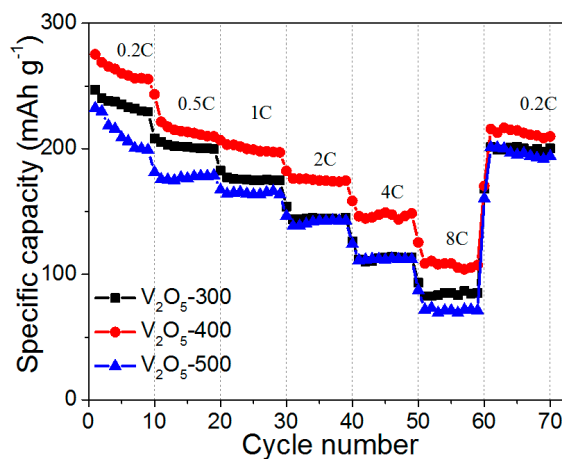


Figure 6. Rate performance of V_2O_5 -300, V_2O_5 -400 and V_2O_5 -500 cathodes.

Electrochemical impedance spectroscopy (EIS) analysis was performed to better understand the rate performance. Figure 7 shows the resulting Nyquist plots of the three cathodes. The Nyquist plots are composed of a depressed semicircle in the high- to medium-frequency region and an inclined line in the low-frequency region [33,34]. The x -intercept on the Z' axis at the very high frequency corresponds to the bulk resistance of the electrode, and this is identical for the three cathodes ($\sim 4 \Omega$), as shown in the inset. The diameter of the semicircle in the high- to medium-frequency region represents the charge-transfer resistance (R_{ct}). The inclined line in the low-frequency region is related to the Li-ion diffusion in the electrode materials. The EIS spectra of the cathodes were obtained in the same frequency range of 10 mHz–100 kHz. It is noted that the V_2O_5 -400 cathode showed much smaller impedance in the low-frequency range, leading to the impedance of no more than 600 Ohms. The R_{ct} of V_2O_5 -400 was estimated to be about 250 Ω , which is much lower than that of V_2O_5 -300 (450 Ω) and V_2O_5 -500 (1250 Ω). The reduced R_{ct} could afford fast reaction kinetics for the Li-ion intercalation-deintercalation in the V_2O_5 -400 cathode, thereby rendering an excellent rate capability.

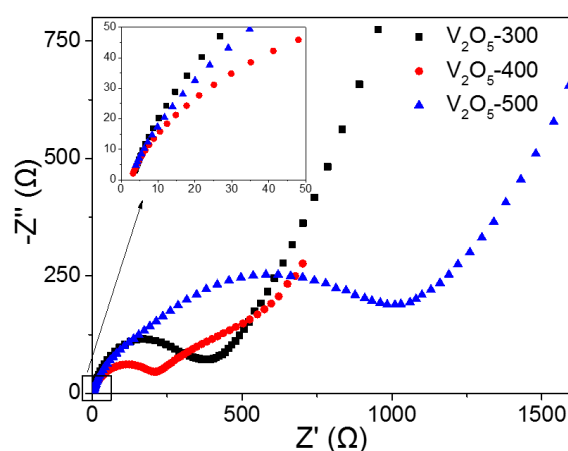


Figure 7. The Nyquist plots of V_2O_5 -300, V_2O_5 -400 and V_2O_5 -500 cathodes (inset is the enlarged part).

The good electrochemical performance of the V_2O_5 -400 cathode can be ascribed to the unique hollow structure of the microspheres [9,29]. First, the nanoscale thickness of the shells can shorten the ion/electron transport distance for rapid charge transfer reactions; Second, the hollow space within the microspheres facilitates adequate electrolyte penetration and enlarges the effective contact area of the electrode/electrolyte interfaces; Third, the hollow structure could accommodate the volume change of V_2O_5 during the electrochemical processes, thus ensuring the good structural integrity of the electrode. In addition, the superior performance of V_2O_5 -400 cathode can be ascribed to the moderate annealing temperature (400 $^{\circ}C$) that renders high crystallinity of bulk materials and a uniform nanoparticle-assembled shell structure.

3. Materials and Methods

Materials Synthesis: V_2O_5 precursor microspheres were prepared by a solvothermal method. In a typical synthesis procedure, NH_4VO_3 (0.9 g) and poly(ethylene oxide)-block-poly(propylene oxide)-blockpoly(ethylene oxide) copolymer (P123) (1.5 g, $Mw = 5800$) and 6 mL of $2 \text{ mol}\cdot\text{L}^{-1}$ HCl were first dissolved in 90 mL of absolute ethanol under stirring. The clear mixture solution was then transferred to a Teflon-lined autoclave and solvothermally treated at 200 $^{\circ}C$ for 24 h. The precipitates were filtered and washed thoroughly with distilled water. Subsequently, the as-collected V_2O_5 precursor microspheres were annealed at 300, 400, and 500 $^{\circ}C$ for 2 h in air to obtain the final V_2O_5 -300, V_2O_5 -400, and V_2O_5 -500 samples, respectively.

Materials Characterization: the phase structure information was obtained by X-ray diffraction (XRD, X'Pert Pro MPD, Philips, Almelo, The Netherlands) with $Cu\text{-}k\alpha$ radiation (1.5418 \AA). The Raman

spectrum was collected by Renishaw Invia RM200 (London, UK) in the spectral range of 90–1200 cm^{-1} . The morphology of the samples was observed by a field emission scanning electron microscopy (FE-SEM, NanoSEM 450, FEI, Portland, OR, USA).

Electrochemical Measurements: the working electrodes were prepared by mixing active materials, carbon black, and PVDF (in a weight ratio of 70:20:10). The mixture slurry was uniformly pasted on the Al foil with a blade. The slurry-coated Al foil was dried at 120 °C in a vacuum oven overnight, followed by punching into circular electrodes with a diameter of 12 mm. The thickness of the cathode without Al foil is about 35 μm , which is more thicker than most of V_2O_5 -based cathodes. Electrochemical measurements were carried out using coin-type cells (CR2032). Lithium plates were used as the counter electrode, and a 1 M solution of LiPF_6 in ethylene carbon (EC)/dimethyl carbonate (DMC)/diethyl carbonate (1:1:1 $w/w/w$) was used as the electrolyte. Cyclic voltammetry (CV) and electrochemical impedance spectroscopy (EIS) were tested with a Solartron electrochemical workstation (1260 + 1287, Bognor Regis, UK). Galvanostatic charge/discharge cycling test was conducted using a Land Battery Testing system (Land, Wuhan, China). The specific capacities are calculated based on the mass of the active material.

4. Conclusions

In summary, V_2O_5 hollow microspheres were solvothermally synthesized by using P123 surfactant as the soft template and NH_4VO_3 as the low-cost vanadium source. The hollow-structured V_2O_5 can serve as an excellent cathode material for lithium-ion batteries, and it delivers a specific capacity as high as 273 $\text{mAh}\cdot\text{g}^{-1}$, a high-rate capacity of 114 $\text{mAh}\cdot\text{g}^{-1}$ at 8 C and good cycling stability. The superior electrochemical properties can be attributed to the unique hollow structure that promotes the electronic/ionic transport and accommodates the structural change. The present study also demonstrates that V_2O_5 hollow microspheres can be a promising alternative cathode material for next-generation lithium-ion batteries.

Acknowledgments: The authors acknowledge the financial support of this work by the National Natural Science Foundation of China (51402236, 51472204, 51302219), the Natural Science Foundation of Shanxi Province (2015JM5180), the Research Fund of the State Key Laboratory of Solidification Processing (NWPU), China (Grant No.: 123-QZ-2015), the Key Laboratory of New Ceramic and Fine Processing (Tsinghua University, KF201607), the Seed Foundation of Innovation and Creation for Graduate Students in Northwestern Polytechnical University (Z2016067) and the Fundamental Research Funds for the Central Universities (3102015BJ(II)MYZ02).

Author Contributions: J.-G.W. conceived the concept. X.Z., H.L., and H.L. carried out the experiments. J.-G.W., X.Z. and B.W. analyzed the results and co-wrote this paper. All the authors made comments to the paper.

Conflicts of Interest: The authors declare no conflict of interest. The founding sponsors had no role in the design of the study; in the collection, analyses, or interpretation of data; in the writing of the manuscript, and in the decision to publish the results.

References

1. Cheng, F.; Liang, J.; Tao, Z.; Chen, J. Functional materials for rechargeable batteries. *Adv. Mater.* **2011**, *23*, 1695–1715. [[CrossRef](#)] [[PubMed](#)]
2. Lu, L.; Han, X.; Li, J.; Hua, J.; Ouyang, M. A review on the key issues for lithium-ion battery management in electric vehicles. *J. Power Sources* **2013**, *226*, 272–288. [[CrossRef](#)]
3. Wang, J.-G.; Kang, F.; Wei, B. Engineering of MnO_2 -based nanocomposites for high performance supercapacitors. *Prog. Mater. Sci.* **2015**, *74*, 51–124. [[CrossRef](#)]
4. Scrosati, B.; Garche, J. Lithium batteries: Status, prospects and future. *J. Power Sources* **2010**, *195*, 2419–2430. [[CrossRef](#)]
5. Kong, L.; Taniguchi, I. Correlation between porous structure and electrochemical properties of porous nanostructured vanadium pentoxide synthesized by novel spray pyrolysis. *J. Power Sources* **2016**, *312*, 36–44. [[CrossRef](#)]

6. Wang, J.-G.; Jin, D.; Zhou, R.; Li, X.; Liu, X.-R.; Shen, C.; Xie, K.; Li, B.; Kang, F.; Wei, B. Highly Flexible Graphene/Mn₃O₄ Nanocomposite Membrane as Advanced Anodes for Li-Ion Batteries. *ACS Nano* **2016**, *10*, 6227–6234. [[CrossRef](#)] [[PubMed](#)]
7. An, Q.; Wei, Q.; Zhang, P.; Sheng, J.; Hercule, K.M.; Lv, F.; Wang, Q.; Wei, X.; Mai, L. Three-dimensional interconnected vanadium pentoxide nanonetwork cathode for high-rate long-life lithium batteries. *Small* **2015**, *11*, 2654–2660. [[CrossRef](#)] [[PubMed](#)]
8. Wang, J.-G.; Jin, D.; Liu, H.; Zhang, C.; Zhou, R.; Shen, C.; Xie, K.; Wei, B. All-manganese-based Li-ion batteries with high rate capability and ultralong cycle life. *Nano Energy* **2016**, *22*, 524–532. [[CrossRef](#)]
9. Wu, H.B.; Pan, A.; Hng, H.H.; Lou, X.W.D. Template-assisted formation of rattle-type V₂O₅ hollow microspheres with enhanced lithium storage properties. *Adv. Funct. Mater.* **2013**, *23*, 5669–5674. [[CrossRef](#)]
10. Zhou, X.; Cui, C.; Wu, G.; Yang, H.; Wu, J.; Wang, J.; Gao, G. A novel and facile way to synthesize vanadium pentoxide nanospire as cathode materials for high performance lithium ion batteries. *J. Power Sources* **2013**, *238*, 95–102. [[CrossRef](#)]
11. McNulty, D.; Buckley, D.N.; O'Dwyer, C. Synthesis and electrochemical properties of vanadium oxide materials and structures as li-ion battery positive electrodes. *J. Power Sources* **2014**, *267*, 831–873. [[CrossRef](#)]
12. Su, Y.; Pan, A.; Wang, Y.; Huang, J.; Nie, Z.; An, X.; Liang, S. Template-assisted formation of porous vanadium oxide as high performance cathode materials for lithium ion batteries. *J. Power Sources* **2015**, *295*, 254–258. [[CrossRef](#)]
13. Wu, H.; Qin, M.; Li, X.; Cao, Z.; Jia, B.; Zhang, Z.; Zhang, D.; Qu, X.; Volinsky, A.A. One step synthesis of vanadium pentoxide sheets as cathodes for lithium ion batteries. *Electrochim. Acta* **2016**, *206*, 301–306. [[CrossRef](#)]
14. An, Q.; Zhang, P.; Xiong, F.; Wei, Q.; Sheng, J.; Wang, Q.; Mai, L. Three-dimensional porous V₂O₅ hierarchical octahedrons with adjustable pore architectures for long-life lithium batteries. *Nano Res.* **2015**, *8*, 481–490. [[CrossRef](#)]
15. Bruce, P.G.; Scrosati, B.; Tarascon, J.M. Nanomaterials for rechargeable lithium batteries. *Angew. Chem. Int. Ed. Engl.* **2008**, *47*, 2930–2946. [[CrossRef](#)] [[PubMed](#)]
16. Huang, S.-Z.; Cai, Y.; Jin, J.; Li, Y.; Zheng, X.-F.; Wang, H.-E.; Wu, M.; Chen, L.-H.; Su, B.-L. Annealed vanadium oxide nanowires and nanotubes as high performance cathode materials for lithium ion batteries. *J. Mater. Chem. A* **2014**, *2*, 14099. [[CrossRef](#)]
17. Wang, J.; Cui, C.; Gao, G.; Zhou, X.; Wu, J.; Yang, H.; Li, Q.; Wu, G. A new method to prepare vanadium oxide nano-urchins as a cathode for lithium ion batteries. *RSC Adv.* **2015**, *5*, 47522–47528. [[CrossRef](#)]
18. Li, Z.; Liu, G.; Guo, M.; Ding, L.-X.; Wang, S.; Wang, H. Electrospun porous vanadium pentoxide nanotubes as a high-performance cathode material for lithium-ion batteries. *Electrochim. Acta* **2015**, *173*, 131–138. [[CrossRef](#)]
19. Tang, W.; Gao, X.; Zhu, Y.; Yue, Y.; Shi, Y.; Wu, Y.; Zhu, K. A hybrid of V₂O₅ nanowires and mwcnts coated with polypyrrole as an anode material for aqueous rechargeable lithium batteries with excellent cycling performance. *J. Mater. Chem.* **2012**, *22*, 20143–20145. [[CrossRef](#)]
20. Liu, H.; Yang, W. Ultralong single crystalline V₂O₅ nanowire/graphene composite fabricated by a facile green approach and its lithium storage behavior. *Energy Environ. Sci.* **2011**, *4*, 4000–4008. [[CrossRef](#)]
21. Mai, L.; Dong, F.; Xu, X.; Luo, Y.; An, Q.; Zhao, Y.; Pan, J.; Yang, J. Cucumber-like V₂O₅/poly(3,4-ethylenedioxythiophene)&MnO₂ nanowires with enhanced electrochemical cyclability. *Nano Lett.* **2013**, *13*, 740–745. [[PubMed](#)]
22. Lee, M.; Balasingam, S.K.; Jeong, H.Y.; Hong, W.G.; Lee, H.B.; Kim, B.H.; Jun, Y. One-step hydrothermal synthesis of graphene decorated V₂O₅ nanobelts for enhanced electrochemical energy storage. *Sci. Rep.* **2015**, *5*, 8151. [[CrossRef](#)] [[PubMed](#)]
23. Niu, C.; Li, J.; Jin, H.; Shi, H.; Zhu, Y.; Wang, W.; Cao, M. Self-template processed hierarchical V₂O₅ nanobelts as cathode for high performance lithium ion battery. *Electrochim. Acta* **2015**, *182*, 621–628. [[CrossRef](#)]
24. Qin, M.; Liang, Q.; Pan, A.; Liang, S.; Zhang, Q.; Tang, Y.; Tan, X. Template-free synthesis of vanadium oxides nanobelt arrays as high-rate cathode materials for lithium ion batteries. *J. Power Sources* **2014**, *268*, 700–705. [[CrossRef](#)]
25. Chao, D.; Xia, X.; Liu, J.; Fan, Z.; Ng, C.F.; Lin, J.; Zhang, H.; Shen, Z.X.; Fan, H.J. A V₂O₅/conductive-polymer core/shell nanobelt array on three-dimensional graphite foam: A high-rate, ultrastable, and freestanding cathode for lithium-ion batteries. *Adv. Mater.* **2014**, *26*, 5794–5800. [[CrossRef](#)] [[PubMed](#)]

26. Chen, M.; Xia, X.; Yuan, J.; Yin, J.; Chen, Q. Free-standing three-dimensional continuous multilayer V₂O₅ hollow sphere arrays as high-performance cathode for lithium batteries. *J. Power Sources* **2015**, *288*, 145–149. [[CrossRef](#)]
27. Ren, X.C.; Zhai, Y.J.; Zhu, L.; He, Y.Y.; Li, A.H.; Guo, C.L.; Xu, L.Q. Fabrication of various V₂O₅ hollow microspheres as excellent cathode for lithium storage and the application in full cells. *ACS Appl. Mater. Interfaces* **2016**, *8*, 17205–17211. [[CrossRef](#)] [[PubMed](#)]
28. Yu, X.-Y.; Yu, L.; Lou, X.W.D. Metal sulfide hollow nanostructures for electrochemical energy storage. *Adv. Energy. Mater.* **2016**, *6*, 1501333. [[CrossRef](#)]
29. Kim, T.; Shin, J.; You, T.-S.; Lee, H.; Kim, J. Thermally controlled V₂O₅ nanoparticles as cathode materials for lithium-ion batteries with enhanced rate capability. *Electrochim. Acta* **2015**, *164*, 227–234. [[CrossRef](#)]
30. Guo, Y.; Li, J.; Chen, M.; Gao, G. Facile synthesis of vanadium pentoxide@carbon core-shell nanowires for high-performance supercapacitors. *J. Power Sources* **2015**, *273*, 804–809. [[CrossRef](#)]
31. Cao, Z.; Wei, B. V₂O₅/single-walled carbon nanotube hybrid mesoporous films as cathodes with high-rate capacities for rechargeable lithium ion batteries. *Nano Energy* **2013**, *2*, 481–490. [[CrossRef](#)]
32. Li, G.; Qiu, Y.; Hou, Y.; Li, H.; Zhou, L.; Deng, H.; Zhang, Y. Synthesis of V₂O₅ hierarchical structures for long cycle-life lithium-ion storage. *J. Mater. Chem. A* **2015**, *3*, 1103–1109. [[CrossRef](#)]
33. Wang, J.-G.; Zhang, C.; Jin, D.; Xie, K.; Wei, B. Synthesis of ultralong MnO/C coaxial nanowires as freestanding anodes for high-performance lithium ion batteries. *J. Mater. Chem. A* **2015**, *3*, 13699–13705. [[CrossRef](#)]
34. Sun, B.; Huang, K.; Qi, X.; Wei, X.; Zhong, J. Rational construction of a functionalized V₂O₅ nanosphere/mwcnt layer-by-layer nanoarchitecture as cathode for enhanced performance of lithium-ion batteries. *Adv. Funct. Mater.* **2015**, *25*, 5633–5639. [[CrossRef](#)]



© 2017 by the authors; licensee MDPI, Basel, Switzerland. This article is an open access article distributed under the terms and conditions of the Creative Commons Attribution (CC BY) license (<http://creativecommons.org/licenses/by/4.0/>).